Acta Oceanol. Sin., 2023, Vol. 42, No. 8, P. 134–146
https://doi.org/10.1007/s13131-023-2146-1
http://www.aosocean.com
E-mail: ocean2@hyxb.org.cn

Features and factors of radium isotopes in Tianjin's typical estuaries

Zhe Zhang[1], Yingchun Dong[1], Lixin Yi[1]*, Xin Hao[1], Yajie Zheng[1], Tianxue Lü[1]

[1] College of Environmental Science and Engineering, Nankai University, Tianjin 300350, China

Received 19 October 2022; accepted 28 January 2023

Abstract

In order to characterize the features of radium isotopes in estuaries of Tianjin, a continuous survey and sampling of typical estuaries were conducted from 2013 to 2017 in this study. The activities of natural radioactive radium isotopes (^{223}Ra, ^{224}Ra, and ^{228}Ra) in groundwater and surface water were measured by the radium-delayed coincidence counting (RaDeCC) system. The non-conservative behavior of the radium isotopes was investigated under hydrogeochemical conditions and urbanization. The results indicated that in terms of horizontal distribution, the activities of radium in groundwater (Hangu, Tanggu, and Dagang) showed an upward trend from north to south and demonstrated a higher figure than surface water (Haihe River and Duliujian River). Concerning the vertical distribution, the activitives of radium at a 15 m burial depth was higher than that at a 30 m burial depth in all measurements. The activities of radium isotopes in the study area increased with the increase of total dissolved solids, and their desorption behavior on Fe-Mn oxides was constrained by the redox intensity. Different hydrogeological conditions resulted in variations in the vertical profile of radium activities. The activity of radium was regulated by seasonal variation and precipitation in groundwater and surface water. In addition, the rapid urbanization has caused a significant impact on the features of radium isotopes in typical estuaries of Tianjin. Meanwhile, radium isotopes can be applied to reflect the impact of urbanization on surface water-groundwater systems. Clarifying and cleverly utilizing the relationship between behavior of radium isotopes and urbanization will promote the development of the Tianjin Binhai New Area in a healthy way.

Key words: estuary, radium isotope, total dissolved solids, ionic strength, urbanization

Citation: Zhang Zhe, Dong Yingchun, Yi Lixin, Hao Xin, Zheng Yajie, Lü Tianxue. 2023. Features and factors of radium isotopes in Tianjin's typical estuaries. Acta Oceanologica Sinica, 42(8): 134–146, doi: 10.1007/s13131-023-2146-1

1 Introduction

The estuarine and coastal zone is an essential economic, social and ecological region. With China's rapid urbanization, the hydrogeochemical environment of the coastal area has been seriously affected. However, the increasing deterioration of the estuarine and coastal zone ecological environment, in turn, inhibits the development of society (Liu et al., 2007). Therefore, it is crucial to conduct studies on the impact of human activities on the coastal environment for regional environmental governance and management.

The behavior of radium isotopes in the hydrogeochemical environment can be a good indicator of the urbanization process. Therefore, the process of urbanization can be indirectly reflected by studying the features of radium isotopes in surface water and groundwater (Tang et al., 2015). The four natural radioisotopes of radium are ^{226}Ra (half-life period $T_{1/2}$ = 1 600 a), ^{228}Ra ($T_{1/2}$ = 5.75 a), ^{224}Ra ($T_{1/2}$ = 3.66 d), and ^{223}Ra ($T_{1/2}$ = 11.4 d), which are produced by the radioactive decay of uranium (^{238}U and ^{235}U) and thorium (^{232}Th) isotopes. Their different half-lives and sources present different geochemical behaviors in aqueous environments (Garcia-Orellana et al., 2021).

Elsinger and Moore (1980) found that ionic strength altered the adsorption and desorption behaviors of radium isotopes in estuarine and coastal zone. The features of radium isotopes in the estuaries are closely related to the ionic strength, which was also confirmed in the studies of Plater et al. (1995) and Vinson et al. (2013). Redox may be an important factor regulating the features of radium isotopes in estuaries by constraining the presence of metal oxides (such as Fe-Mn oxides) (Charette and Sholkovitz, 2002; Tang et al., 2015). In groundwater, aquifer rock types, mineral weathering and co-precipitation play an important role in regulating the distribution of radium. For example, Shao et al. (2009) pointed out that montmorillonite and barite have different migration behaviors of radium isotopes in groundwater through numerical simulation. Therefore, the activity level of radium isotopes in groundwater will be jointly affected by the physical and chemical processes and hydrological environment, including adsorption-desorption, redox, hydrolysis-co-precipitation, and other aquatic environmental indicators (such as temperature, salinity, total dissolved solids (TDS), and pH, etc.). The behavior of radium isotopes in surface water and groundwater systems are influenced by physicochemical processes and hydrogeology.

On the other hand, based on the difference in radium isotope activities between surface water and groundwater, radium isotope has been widely used in studying this system under urbanization process (IAEA, 2014; Charette et al., 2015). For instance, the water retention time of estuarine and coastal zone directly affects the productivity, it is proposed that the application of radium isotope to consider water residence time in this area can help

Foundation item: The National Natural Science Foundation of China under contract No. 42172273.
*Corresponding author, E-mail: yilixin@nankai.edu.cn

to evaluate the metabolic rate of the water ecosystem and indirectly reflect the pollution self-purification ability of the water (Moore, 2000a, b). In addition, studies estimating submarine groundwater discharge (SGD) fluxes in estuarine and coastal zone based on the mass balance of radium isotopes have been reported more frequently (Kelly and Moran, 2002; Luo et al., 2014). In summary, radium isotopes can also be a good indicator of hydrogeochemical processes under urbanization.

It is common to analyze the non-conservative behavior of radium isotopes in estuarine and coastal zones based on hydrogeological conditions. However, the impact of rapid urbanization is rarely considered. This study selected the typical estuaries of Tianjin affected by human activities as the research objects, including groundwater (Hangu (HG), Tanggu (TG), and Dagang (DG)) and surface water (Haihe River (HH) and Duliujian River (DLJ)). The horizontal and vertical distribution characteristics of radium isotope activities in surface water and groundwater were analyzed. Finally, we further explored the behavior of radium isotopes in the hydrogeochemical environment and urbanization process. Clarifying and skillfully utilizing the relationship between behavior of radium isotopes and urbanization will actively promote the healthy development of the Tianjin Binhai New Area.

2 Sampling and measurement

The investigation area is located in Binhai New Area, Tianjin, which is close to the Bohai Bay (Fig. 1). A total of 28 field sampling surveys were conducted. The samples of the groundwater (HG, TG, and DG) were collected from pumping wells at depths of 15 m and 30 m, respectively, in May and September 2017. The surface water (HH and DLJ) samples were collected at a depth of 1 m from March 2013 to November 2015. All samples were stored in 25 L plastic buckets (made of high density polyethylene), with a total volume of 50 L for water samples. They were brought back to the laboratory for determination within 24 h.

In the laboratory, all samples went through the necessary filtration and enrichment. First, we used cellulose acetate membrane (pore size: 0.45 μm) to filter in order to exclude the influence of impurities such as suspended particles on the enrichment of MnO_2 fibers, and then place the filtered water samples on a high platform with samples containing 20 g of dry MnO_2 fibers. Secondly, based on the siphon principle, we controlled the water sample to pass through the sample column at a flow rate of about 1 L/min to complete the extraction of radium isotopes, and

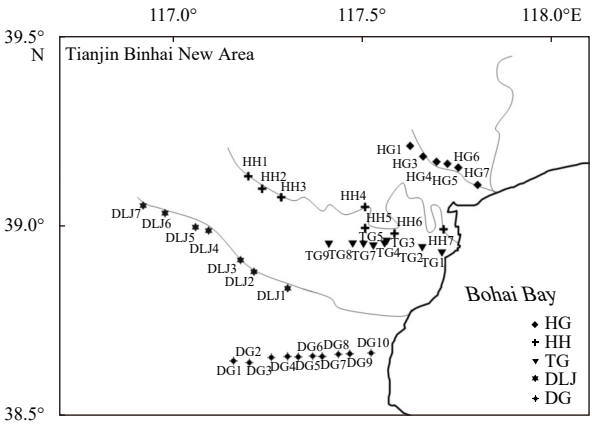

Fig. 1. The scope of the study area and sampling stations. HG: Hangu; TG: Tanggu; DG: Dagang; HH: Haihe River; DLJ: Duliujian River.

the extraction efficiency was as high as 98% (Moore and Arnold, 1996; Moore et al., 1985). Finally, the enriched MnO_2 fiber was cleaned with deionized water to remove the salt and solid particles attached to the surface of the MnO_2 fiber. The water content of MnO_2 fiber was adjusted by vacuum pump (75% of the dry MnO_2 fiber mass (20 g)), so that the total treated MnO_2 fiber was (35.0±0.1) g (Moore, 2008).

To avoid decay affecting the results, the ^{224}Ra activity of samples was determined within 1–3 d (the first measurement). The activity of ^{223}Ra was affected by the alpha signal produced by the radioactive decay of ^{224}Ra and its progeny, so the measurement of ^{223}Ra was performed within 7–9 d (the second measurement) (Moore, 2008; Moore and Arnold, 1996). Since ^{228}Th in water samples was also adsorbed on the MnO_2 fibers while samples were being filtered, the ^{228}Th activity was measured in the fourth week (the third measurement) after sampling to correct the ^{224}Ra activity. At this point, ^{224}Ra and ^{228}Th have reached the decay equilibrium, and then we conducted the third measurement to obtain the contribution of ^{228}Th to ^{224}Ra in the sample. Finally, this study combined the results of the first measurement to obtain the corrected ^{224}Ra activity. After three measurements, the samples were sealed for 10–12 months for the fourth measurement, the ^{228}Th decay on the MnO_2 fibers was completed and the activity of ^{228}Ra has been determined (Moore, 2008). The computational errors of ^{224}Ra, ^{228}Ra, and ^{223}Ra are approximately 6%, 7.5%, and 10%, respectively (Moore and Arnold, 1996; Waska et al., 2008). In this study, the concentration of cations (Ca^{2+}, Mg^{2+}, Na^{+} and K^{+}) was determined by inductively coupled plasma optical emission spectrometer (ICP-OES, Platinum Elmer Inc., USA), with an error of ±5%, while the concentration of anions (SO_4^{2-}, NO_3^{-} and Cl^{-}) is determined by ion chromatographs (ICS-2 100, Diane, USA) with an error of ±6%. The concentration of HCO_3^{-} was measured by titration with an error of ±5%.

3 Results

3.1 *Radium in groundwater*

Radium activities of HG, TG, and DG in spring and autumn are presented in Table 1. The results indicated that the variation range of radium activities in groundwater is extensive, reaching 2–3 orders of magnitude, mainly due to the different lithology of the aquifer in the groundwater environment (Moore et al., 1995; Moore, 1996). The spring's average activities of ^{223}Ra, ^{224}Ra and ^{228}Ra in the HG (15 m buried depth, the same as below) were 4.14 dpm/(100 L) (1 Bq=60 dpm), 286.91 dpm/(100 L), and 140.96 dpm/(100 L), respectively. The average activities of ^{223}Ra, ^{224}Ra and ^{228}Ra in the TG were 18.40 dpm/(100 L), 267.74 dpm/(100 L), and 240.88 dpm/(100 L), respectively. The average activities of ^{223}Ra, ^{224}Ra and ^{228}Ra in the DG were 142.05 dpm/(100 L), 2 110.91 dpm/(100 L), and 907.77 dpm/100 L, respectively. The activities of radium in spring were HG<TG<DG, while the autumn is different from spring. The average activities of ^{223}Ra, ^{224}Ra and ^{228}Ra in the HG were 5.46 dpm/(100 L), 165.70 dpm/(100 L), and 161.18 dpm/(100 L) in autumn, respectively. The average activities of ^{223}Ra, ^{224}Ra and ^{228}Ra were 3.02 dpm/(100 L), 103.20 dpm/(100 L), and 82.02 dpm/(100 L) in the TG, respectively. The average activities of ^{223}Ra, ^{224}Ra and ^{228}Ra in the DG were 31.32 dpm/(100 L), 879.31 dpm/(100 L), and 889.40 dpm/(100 L), respectively. The activities of radium in water in autumn were TG<HG<DG. As a result, groundwater radium activities were affected by seasonal variation (Underwood et al., 2009).

3.2 *Radium in surface water and the difference with groundwater*

Table 2 shows the radium activities of HH and DLJ in differ-

Table 1. Measurements of ^{223}Ra, ^{224}Ra and ^{228}Ra in groundwater

Sample	Depth/m	Latitude	Longitude	^{223}Ra/(dpm·(100 L)$^{-1}$)		^{224}Ra/(dpm·(100 L)$^{-1}$)		^{228}Ra/(dpm·(100 L)$^{-1}$)	
				Spring	Autumn	Spring	Autumn	Spring	Autumn
HG1	15	39.21°N	117.63°E	3.18	1.07	35.22	21.92	23.61	35.97
HG3	15	39.18°N	117.66°E	0.28	0.57	26.97	41.07	3.61	40.31
HG4	15	39.17°N	117.67°E	0.13	–	31.30	–	11.12	–
HG4	30	39.17°N	117.67°E	0.26	–	9.03	–	6.71	–
HG5	15	39.16°N	117.67°E	5.61	17.78	383.21	503.87	201.48	332.40
HG6	15	39.15°N	117.69°E	5.68	–	631.97	–	374.02	–
HG6	30	39.15°N	117.69°E	0.24	–	56.28	–	64.14	–
HG7	15	39.15°N	117.70°E	9.93	2.44	612.76	95.93	231.90	236.06
TG1	15	38.93°N	117.67°E	10.53	–	209.42	–	425.16	–
TG2	15	38.94°N	117.66°E	5.87	–	138.73	–	416.04	–
TG3	15	38.95°N	117.65°E	102.94	–	618.67	–	488.19	–
TG3	30	38.95°N	117.65°E	1.49	24.74	65.34	1 936.98	36.57	32.61
TG4	15	38.95°N	117.63°E	22.99	–	885.81	–	310.46	–
TG5	15	38.95°N	117.61°E	1.34	9.94	80.45	317.81	72.22	169.45
TG5	30	38.95°N	117.61°E	2.31	0.89	3 384.80	104.72	1 099.93	23.24
TG7	15	38.97°N	117.56°E	0.66	0.52	63.47	17.42	93.21	33.73
TG8	15	38.99°N	117.53°E	1.20	1.49	40.92	52.20	55.61	55.11
TG8	30	38.99°N	117.53°E	7.49	–	289.43	–	340.15	–
TG9	15	39.00°N	117.47°E	1.68	0.11	104.48	25.38	66.16	69.78
DG1	15	38.64°N	117.38°E	38.41	12.80	976.90	448.77	809.54	236.07
DG1	30	38.64°N	117.38°E	3.51	0.01	132.69	11.68	100.23	13.61
DG2	15	38.64°N	117.40°E	113.35	40.24	2 702.10	906.58	949.95	904.35
DG3	15	38.65°N	117.44°E	70.22	1.06	1 383.59	71.15	623.95	456.40
DG4	15	38.66°N	117.47°E	64.15	66.05	1 489.13	1 563.82	471.53	928.50
DG4	30	38.66°N	117.47°E	3.12	2.79	86.04	111.23	65.22	318.54
DG5	15	38.66°N	117.49°E	321.64	61.40	3 022.17	1 814.50	1 047.14	1 063.86
DG5	30	38.66°N	117.49°E	2.74	4.45	58.27	126.65	63.36	573.35
DG6	15	38.66°N	117.51°E	356.12	61.55	3 281.96	1 846.62	1 452.83	1 810.29
DG7	30	38.66°N	117.52°E	357.64	1.59	3 026.60	182.59	1 100.73	198.41
DG7	15	38.66°N	117.52°E	2.48	15.92	198.73	947.32	332.17	1 035.72
DG8	15	38.66°N	117.56°E	314.88	11.17	4 276.96	214.62	2 004.84	572.41
DG9	15	38.66°N	117.55°E	47.34	24.28	1 671.79	552.71	639.33	825.89
DG9	30	38.66°N	117.55°E	10.32	4.51	314.65	173.82	415.58	495.18
DG10	15	38.67°N	117.54°E	91.89	18.79	2 105.74	426.99	766.39	1 060.53

Note: HG: Hangu; TG: Tanggu; DG: Dagang. – represents no data.

Table 2. Measurements of ^{223}Ra, ^{224}Ra and ^{228}Ra in surface water

Station	Latitude	Longitude	^{223}Ra/(dpm·(100 L)$^{-1}$)			^{224}Ra/(dpm·(100 L)$^{-1}$)			^{228}Ra/(dpm·(100 L)$^{-1}$)		
			Spring	Summer	Autumn	Spring	Summer	Autumn	Spring	Summer	Autumn
HH1	39.13°N	117.20°E	0.24	0.31	0.39	7.06	10.16	7.64	11.39	15.15	7.41
HH2	39.10°N	117.24°E	0.34	0.36	0.38	4.55	8.76	6.25	8.95	13.56	7.53
HH3	39.08°N	117.29°E	0.38	0.29	0.43	6.92	9.04	8.57	10.75	24.95	9.59
HH4	39.05°N	117.51°E	0.11	0.29	0.41	5.20	10.43	8.04	14.07	10.45	9.12
HH5	38.99°N	117.51°E	0.46	0.73	0.70	17.05	17.35	12.20	50.68	35.65	34.67
HH6	38.98°N	117.58°E	0.79	0.54	0.84	17.10	18.30	14.56	59.69	58.07	37.85
HH7	38.99°N	117.71°E	2.13	2.34	2.03	40.43	50.07	45.02	193.13	156.77	188.08
DLJ1	38.84°N	117.30°E	2.02	2.49	1.13	51.75	50.62	23.09	52.11	53.61	41.17
DLJ2	38.88°N	117.21°E	2.79	1.95	1.35	56.38	46.00	31.80	53.48	41.84	39.58
DLJ3	38.91°N	117.18°E	2.08	2.14	1.34	60.20	49.91	25.85	50.85	51.42	37.98
DLJ4	38.99°N	117.09°E	1.59	1.46	1.22	42.58	30.92	27.64	32.28	20.32	27.61
DLJ5	39.00°N	117.06°E	1.95	0.93	0.98	43.54	45.48	22.39	33.34	38.84	22.57
DLJ6	39.03°N	116.98°E	2.25	1.54	0.72	56.04	42.10	20.46	44.32	31.06	19.46
DLJ7	39.05°N	116.92°E	1.08	1.55	0.66	33.07	31.75	15.81	33.85	29.92	18.99

Note: HH: Haihe River; DLJ: Duliujian River.

ent seasons. The results showed that the variations of activity range of radium in the surface water are negligible. The average activities of ^{223}Ra-HH in spring, summer and autumn were 0.64 dpm/(100 L), 0.70 dpm/(100 L), and 0.74 dpm/(100 L), re-

spectively. The average activities of ^{224}Ra-HH were 14.04 dpm/(100 L), 17.73 dpm/(100 L), and 14.61 dpm/(100 L), respectively. The average activities of ^{228}Ra-HH were 49.81 dpm/(100 L), 44.94 dpm/(100 L), and 42.04 dpm/(100 L), respectively. Therefore, the radium activity of HH is less sensitive to seasonal variations.

The radium activity of DLJ varies in different seasons, unlike that of HH. The average activities of ^{223}Ra-DLJ in spring, summer and autumn were 1.97 dpm/(100 L), 1.72 dpm/(100 L), and 1.06 dpm/(100 L), respectively. The average activities of ^{224}Ra-DLJ were 49.08 dpm/(100 L), 42.40 dpm/(100 L), and 23.86 dpm/(100 L), respectively. The average activities of ^{228}Ra-DLJ were 42.89 dpm/(100 L), 38.14 dpm/(100 L), and 29.62 dpm/(100 L), respectively. Therefore, the radium activities of DLJ were autumn < summer < spring. Seasonal variations will also regulate the radium activity of surface water, and different types of surface water have different responses to seasonal variations.

Radium isotopes are widely distributed in different water environments (Langmuir and Melchior, 1985; Charette et al., 2015). Significant differences in radium activity between groundwater and surface water have been found. Radium activity and spatial variability in groundwater were higher than in surface water. It is consistent with previous studies (Ni et al., 2013). Tang et al. (2015) indicated that the activities of radium in groundwater were generally higher than that in surface water in estuarine and coastal zone of Tianjin, this is consistent with our research results, possibly due to the abundant rocks and minerals flowing through the groundwater, and the decay and α recoil of the parent body release a large number of radium isotopes (Sherif et al., 2018). However, the salinity and TDS of surface water are low, and the parent nuclides are relatively few, so radium adsorbed on the surface of suspended particles cannot be released into the water body vastly and rapidly (Kiro et al., 2012; IAEA, 2014).

3.3 *Distribution of physicochemical parameters*

The hydrochemical parameters of groundwater in spring and autumn are presented in Tables 3 and 4. The results showed that the TDS of groundwater differs at different depths in different seasons. In spring, the TDS of HG, TG, and DG (15 m depth, the same as below) were 18 071 mg/L, 42 432 mg/L, and 49 168 mg/L, respectively, while in autumn, the TDS of HG, TG, and DG were 11 999 mg/L, 30 037 mg/L, and 57 196 mg/L, respectively. The high TDS mainly occurred in TG and DG, which may be related to the development and utilization of the salt field industry. The

Table 3. Measurements of chemical concentration parameters in groundwater in spring

Sample	Depth/ m	TDS/ (mg·L^{-1})	K$^+$/ (mg·L^{-1})	Ca^{2+}/ (mg·L^{-1})	Na$^+$/ (mg·L^{-1})	Mg^{2+}/ (mg·L^{-1})	HCO_3^-/ (mg·L^{-1})	SO_4^{2-}/ (mg·L^{-1})	NO_3^-/ (mg·L^{-1})	Cl$^-$/ (mg·L^{-1})
HG1	15	15 678	67	60	11 613	197	1 360	1 250	0.92	1 130
HG3	15	8 824	82	43	4 305	133	930	760	1.29	2 570
HG4	15	6 731	116	103	5 434	284	553	118	0.52	123
HG4	30	4 257	21	26	2 998	62	558	232	0.25	360
HG5	15	34 702	232	187	7 602	357	362	2 860	1.21	23 100
HG6	15	23 180	267	199	3 057	343	412	4 700	0.74	14 200
HG6	30	14 994	161	70	6 949	254	89	740	0.67	6 730
HG7	15	19 313	205	113	2 166	314	585	3 230	0.62	12 700
TG1	15	79 654	481	370	9 682	382	533	14 200	6.60	54 000
TG2	15	52 203	354	351	8 791	399	56	6 550	1.76	35 700
TG3	15	104 833	490	303	5 048	397	293	14 000	2.21	84 300
TG3	30	121 341	532	299	15 089	398	322	13 700	2.36	91 000
TG4	15	22 963	351	69	2017	354	661	4 110	0.81	15 400
TG5	15	58 255	249	339	12 475	389	–	3 900	3.09	40 900
TG5	30	46 801	254	279	10 395	382	10	2 580	1.40	32 900
TG7	15	10 776	35	46	8 523	103	484	870	0.25	714
TG8	15	4 665	19	44	2 849	68	723	520	8.37	433
TG8	30	22 007	141	105	15 683	232	551	412	3.50	4 880
TG9	15	6 103	35	48	3 978	75	755	462	1.97	748
DG1	15	26 912	192	97	6 682	343	841	855	1.86	17 900
DG1	30	16 949	117	21	3 116	339	300	855	0.93	12 200
DG2	15	44 082	299	181	8 850	386	474	2 490	1.29	31 400
DG3	15	28 403	254	112	4 691	376	508	2 460	1.06	20 000
DG4	15	43 380	274	213	8 939	355	218	4 080	0.90	29 300
DG4	30	17 297	65	53	4 542	334	181	1 420	1.00	10 700
DG5	15	70 040	343	313	14 673	379	231	6 100	1.26	48 000
DG5	30	20 207	75	134	6 355	310	72	1 460	0.87	11 800
DG6	15	57 951	344	311	12 980	373	303	4 640	1.23	39 000
DG7	30	59 115	314	301	13 010	377	273	3 340	1.30	41 500
DG7	15	23 947	156	92	10 128	318	82	970	0.97	12 200
DG8	15	80 300	395	264	16 159	374	456	4 650	1.52	58 000
DG9	15	72 836	395	234	14 911	373	122	6 000	1.44	50 800
DG9	30	20 547	239	116	3 800	320	62	1 410	0.83	14 600
DG10	15	43 826	324	198	10 930	367	384	4 420	2.99	27 200

Note: – represents no data. TDS: total dissolved solids.

Table 4. Measurements of chemical concentration parameters in groundwater in autumn

Sample	Depth/ m	TDS/ (mg·L^{-1})	K^+/ (mg·L^{-1})	Ca^{2+}/ (mg·L^{-1})	Na^+/ (mg·L^{-1})	Mg^{2+}/ (mg·L^{-1})	HCO_3^-/ (mg·L^{-1})	SO_4^{2-}/ (mg·L^{-1})	NO_3^-/ (mg·L^{-1})	Cl^-/ (mg·L^{-1})
HG1	15	4 691	47	26	1 274	228	837	1 005	0.52	1 274
HG3	15	6 997	66	46	2 103	172	645	834	1.26	3 130
HG5	15	9 657	76	6	2 848	267	231	1 627	1.15	4 600
HG7	15	26 654	181	50	7 687	909	249	1 698	0.56	15 880
TG3	15	73 568	1 699	847	41 400	8 015	31	1814	2.36	19 760
TG3	30	164 712	1 721	832	44 220	8 546	176	12 034	2.46	97 180
TG5	15	70 196	268	670	19 520	3 749	70	3 376	2.24	42 540
TG5	30	80 081	280	757	20 710	4 257	66	4 870	1.40	49 140
TG7	15	1 935	24	27	549	80	308	333	1.03	612
TG8	15	2 015	11	43	645	41	506	231	4.64	533
TG9	15	2 470	24	26	730	82	376	422	1.88	808
DG1	15	8 701	50	63	2 378	365	181	272	1.76	5 391
DG1	30	1 512	39	32	376	30	37	431	0.83	568
DG2	15	64 348	337	211	17 110	2 960	113	2 836	1.19	40 780
DG3	15	46 939	256	67	12 490	2 066	149	2 660	0.99	29 250
DG4	15	57 208	75	196	16 340	1 661	61	4 074	0.85	34 800
DG4	30	53 374	173	49	14 480	1 848	42	2 541	1.00	34 240
DG5	15	86 353	380	423	22 250	3 193	59	6 718	1.16	53 330
DG5	30	67 421	309	371	17 490	2 447	40	4 004	0.85	42 760
DG6	15	84 240	402	583	22 260	2 173	77	5 094	1.22	53 650
DG7	30	84 254	430	553	22 060	2 996	74	3 700	1.29	54 440
DG7	15	30 442	205	45	8 433	1 055	353	–	0.87	20 350
DG8	15	33 488	281	475	8 621	818	48	3 933	1.44	19 310
DG9	15	94 240	680	8	25 690	3 030	49	7 012	1.50	57 770
DG9	30	38 044	232	145	10 350	1 107	29	1 890	0.93	24 290
DG10	15	66 001	446	220	17 170	2 350	141	5 510	3.01	40 160

Note: – represents no data. TDS: total dissolved solids.

proportion of brines in TG and DG groundwater reaches about 50% and 30%, respectively, which is much higher than that in HG. Land salinization leads to differences in TDS (Xiao et al., 2012).

The concentrations of K^+, Ca^{2+}, Na^+ and Mg^{2+} in spring were 232 mg/L, 167 mg/L, 8 189 mg/L, and 307 mg/L, respectively, which were lower than those in autumn (334 mg/L, 260 mg/L, 13 815 mg/L, and 2 094 mg/L). The concentrations of HCO_3^-, SO_4^{2-}, NO_3^- and Cl^- showed the opposite results, which were higher in spring (416 mg/L, 3 540 mg/L, 2 mg/L, and 24 897 mg/L) than in autumn (190 mg/L, 3 157 mg/L, 1 mg/L, and 28 713 mg/L). It showed that seasonal variation regulates ion concentration to a certain extent. For example, the concentration of cations in spring (dry season) was lower than that in autumn (wet season), which may not be suitable season for crop growth in dry season, and the irrigation demand for groundwater extraction is reduced. The ability of soil salt to be transported by water flow is weakened (Sun et al., 2018). However, the concentration of anions in the dry season was higher than that in autumn, indicating that ion concentration was also regulated by other processes. For instance, the concentration of HCO_3^- is related to the dissolution of carbonate and silicates (Trainer and Heath, 1976); the process of denitrification in groundwater will change the concentration of NO_3^- (Adelana et al., 2020); under the influence of human activities, the shallow groundwater may be polluted by sulfate and chloride ion to a certain extent (Abboud, 2018). Therefore, ion concentrations in groundwater are regulated by complex hydrological and biogeochemical processes.

The cation concentration is $Na^+ > Mg^{2+} > K^+ > Ca^{2+}$, and the anion concentration is $Cl^- > SO_4^{2-} > HCO_3^- > NO_3^-$. A Piper three-line diagram was used to divide the water body based on the different chemical compositions of the water body (Giggenbach, 1988; Lu et al., 2022). The results showed that the chemical type of HG is mainly Cl-Na. Cl-HCO_3-Na type also existed. The chemical type of TG is mainly Cl-Na, and Cl-Mg-Na, Cl-SO_4-Na. Cl-HCO_3-SO_4-Na type also existed. In contrast, the chemical composition and type of DG are relatively concentrated, all of which are Cl-Na, indicating that its hydrodynamic conditions are relatively mild.

4 Discussion

4.1 *Geographical distribution characteristics*

To vividly illustrate the distribution characteristics of radium isotopes in the estuaries, Surfer 15 was used to obtain the bubble maps of ^{223}Ra, ^{224}Ra and ^{228}Ra in HG, TG, and DG (15 m depth) and HH, DLJ in different seasons (Figs 2 and 3).

The ^{223}Ra, ^{224}Ra and ^{228}Ra of HG, TG, and DG in spring was consistent with that in autumn, that is, HG < TG < DG, and showed an increasing trend from north to south. Low TDS and specific water chemistry types (Cl-Na and HCO_3-Na) may have promoted the activity reduction of radium in HG. High TDS increases the desorption capacity of adsorbed radium on aquifer laminae, and the water chemistry type of DG is all Cl-Na, which leads to high activitites of radium in DG. From inland to estuaries, the increasing trend is reflected in the activity of radium in HG and TG, and the activities of radium near inland stations were lower than other stations (about 1.5 km from the coastline). Still, the activities variation of radium in DG was different from radium in HG and TG. The activity of radium in DG showed a trend of increasing and then decreasing from inland to the coastline, with high values occurring at DG5, DG6, and DG7, probably due to a large number of oil fields distributed nearby. Oil exploit-

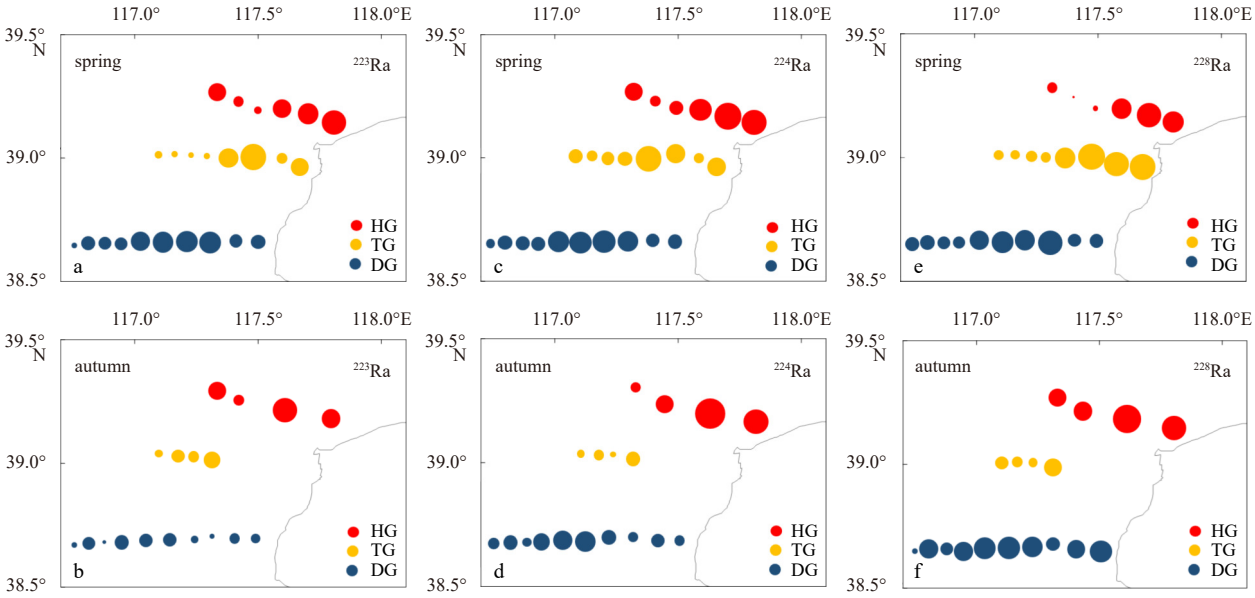

Fig. 2. Horizontal distribution of ^{223}Ra (a, b), ^{224}Ra (c, d) and ^{228}Ra (e, f) activities in groundwater (HG: Hangu; TG: Tanggu; DG: Dagang).

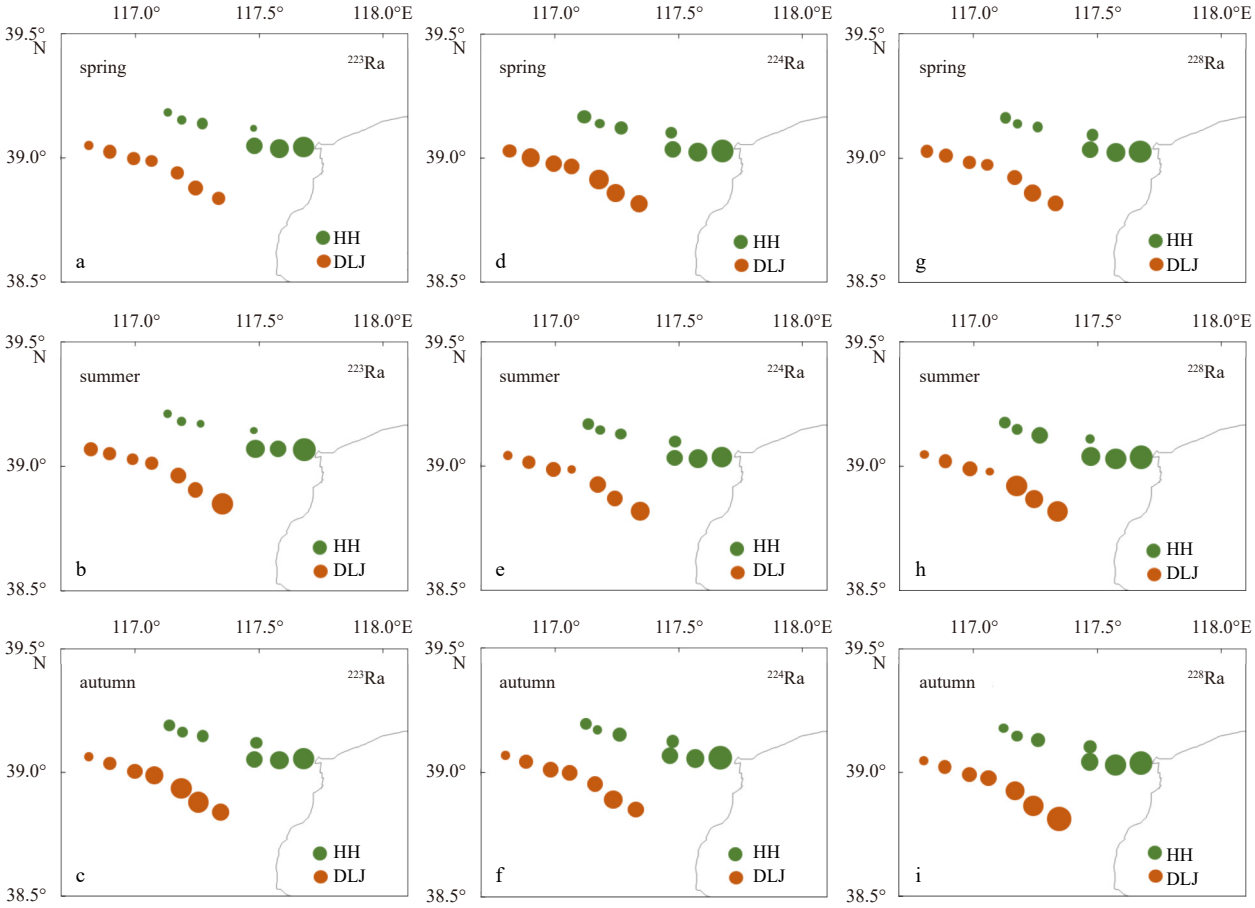

Fig. 3. Horizontal distribution of ^{223}Ra (a–c), ^{224}Ra (d–f) and ^{228}Ra (g–i) activities in surface water (HH: Haihe River; DLJ: Duliujian River).

ation activities lead to the contamination of shallow groundwater, and a large amount of minerals in oil provides a rich parent source of radium in DG.

The distribution of ^{223}Ra, ^{224}Ra and ^{228}Ra in HH and DLJ was consistent in different seasons, showing a trend from low to high from inland to the coastline, with high values occurring in the estuarine zone (HH5, HH6, and HH7; DLJ1, DLJ2, and DLJ3). Figure 4 showed the variation of radium in HH and DLJ with distance. The

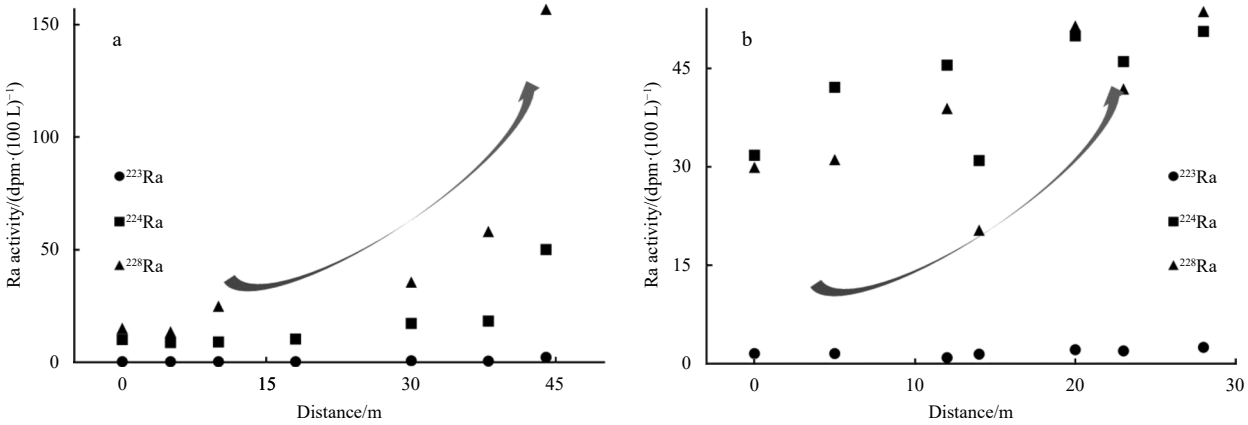

Fig. 4. Activity of ^{223}Ra, ^{224}Ra and ^{228}Ra in surface water (Haihe River (a) and Duliujian River (b)) at each station.

"distance" is linear distance from HH1 and DLJ7 to the rest of the stations, using the upstream river (HH1 and DLJ7) as the origin. It was found that the activities of ^{223}Ra, ^{224}Ra and ^{228}Ra showed a gradual increase from inland to the estuary, although there were slight differences. This demonstrates that the variation of radium activities in estuarine waters is greatly influenced by salinity and TDS with unconservative additive behavior. Elsinger and Moore (1980) indicated that salinity mainly controls the adsorption and desorption of radium isotopes in the estuary (Elsinger and Moore, 1980; van der Loeff et al., 2003) and that the estuary is an essential site for the desorption of radium isotopes (Moore et al., 2006; Beck et al., 2007; Gonneea et al., 2008). HH and DLJ are natural freshwater ecosystems, and radium isotopes are adsorbed on suspended particles and exhibit semi-granular activity. The high TDS in HH and DLJ contributed to the desorption of radium from particulate matter, indicating that the salinity effect was a significant mechanism controlling the migration of radium isotopes. In addition, the hydrochemical environment constrained by human activities and hydrogeological conditions near the estuary also significantly impacts behavior of radium activities (Moore, 2010; Chen et al., 2022).

4.2 *Vertical distribution characteristics*

The vertical distribution characteristics of radium isotopes in different water bodies are of great significance for understanding the hydrodynamic process, vertical recharge flux, and migration time of the region (Liu et al., 2015; Liao et al., 2020; Lu et al., 2022). In spring and autumn, the ^{223}Ra, ^{224}Ra and ^{228}Ra activities at 15 m depth were higher than that at 30 m depth (Fig. 5). The activities of ^{223}Ra, ^{224}Ra and ^{228}Ra in the water at 30 m depth varied in the range of ±2.72 dpm/L, ±84.34 dpm/L, and ±198.02 dpm/(100 L), respectively, while the activities of ^{223}Ra, ^{224}Ra and ^{228}Ra in the water at 15 m depth varied in the range of ±127.54 dpm/L, ±902.79 dpm/L and ±287.36 dpm/(100 L). This may be related to rock properties, aquifer hydrodynamic conditions, and chemical composition (Yi et al., 2019).

4.3 *Factors influencing radium distribution*

In the estuarine and coastal systems, the source terms of radium isotopes mainly include the mineral weathering in the bedrock aquifer, the α recoil of parent nuclides, and the desorption of radium adsorbed on the bedrock surface, river input, and submarine groundwater discharge. The sinks of radium isotopes mainly include their radioactive decay, co-precipitation, and ad-

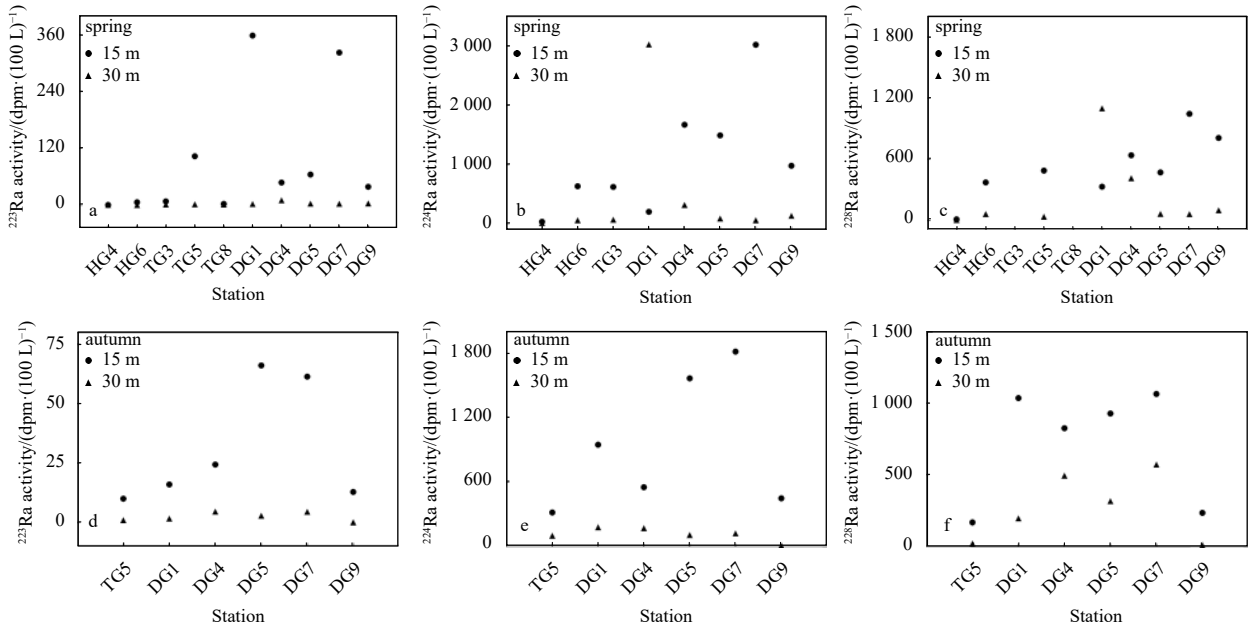

Fig. 5. Groundwater vertical distribution of ^{223}Ra, ^{224}Ra and ^{228}Ra activities in spring (a–c) and autumn (d–f).

sorption (Beck and Cochran, 2013). In addition to the source-sink term, the distribution characteristics of radium are also regulated by the geochemical environment of water bodies, especially ionic strength, redox, hydrogeological conditions, seasonal variations, and urbanization. Therefore, revealing the characteristics of radium isotopes under specific hydrogeological conditions not only helps to understand its migration and transformation patterns in groundwater but also is a prerequisite for using radium isotopes to quantitatively study the environment of groundwater oxidation, groundwater recharge and discharge, and groundwater pollution identification (Grundl and Cape, 2006).

4.3.1 *Ionic strength*

The ionic strength indicates the degree of electrical strength of ions in solution; the higher the number of charges carried by an ion, the higher the ionic strength (Charette and Sholkovitz, 2006). For most natural water bodies, radium in the water column exists mainly in the form of free state Ra^{2+} and is adsorbed by clays and metal oxides. Therefore, ionic strength is an important factor affecting the adsorption and desorption of aqueous radium isotopes at the water-rock interface (Krest and Harvey, 2003).

Figures 6 and 7 showed the relationship between radium isotopes (^{223}Ra, ^{224}Ra and ^{228}Ra) and TDS in different seasons for three aquifers (HG, TG, and DG) and two rivers (HH and DLJ), respectively. In spring and autumn, the ^{223}Ra, ^{224}Ra and ^{228}Ra activities of HG, TG, and DG showed an increasing trend with the increase of TDS, but the growth rate differed. This was consistent with the previous research results (Tang et al., 2015). TDS is an essential indicator for judging the ionic strength of natural water. It has been widely used in studying the source and distribution of radium isotopes in estuarine and coastal areas (Liu et al., 2019). In subsurface aquifers, high TDS promotes the desorption of radium adsorbed on the surface of particulate matter, enhancing the radium activities of HG, TG, and DG. Although there is a positive correlation between radium isotopes and TDS in HG, TG, and DG, the data distribution is scattered. It indicates that other mixing processes (e.g., suspended particulate matter and sediment) also lead to irregularities in the distribution of radium isotopes. The ^{223}Ra, ^{224}Ra and ^{228}Ra activities of HH and DLJ showed a better positive correlation with TDS in spring, summer, and autumn due to the radium isotopes' desorption adsorbed on the suspended particulate matter at the river-sea interface, but the desorption rates were different. ^{223}Ra and ^{224}Ra activities increased more than ^{228}Ra, mainly because the suspended particulate matter of HH and DLJ had ^{223}Ra and ^{224}Ra more than ^{228}Ra and faster regeneration of ^{223}Ra and ^{224}Ra than ^{228}Ra, which is consistent with previous studies on water bodies in estuaries and coastal zones (Liu et al., 2013).

4.3.2 *Redox effects*

There are a lot of inorganic or organic oxidants and reductants in water. The order of oxidizing ability of common oxidants is O_2, NO_3^-, NO_2^-, SO_4^{2-}, S. Vinson et al. (2013) proposed that the existence of NO_3^- and SO_4^{2-} can improve the stability of Fe-Mn oxides at the thermodynamic level (Vinson et al., 2013). Fe-Mn oxides are widely distributed in underground estuaries and have a strong affinity for radium in water, which can hinder the desorption of radium in sediments (Charette and Sholkovitz, 2002). Therefore, the redox environment will indirectly affect the activities of radium isotopes in water.

The radium isotope activity in spring and autumn was mainly distributed in NO_3^- from 0 mg/L to 3 mg/L, with no significant seasonal differences (Fig. 8). Precisely, the radium isotope activity increased at NO_3^- of 0 mg/L to 1 mg/L and decreased at NO_3^- of 1 mg/L to 3 mg/L. Once NO_3^- in the water exceeded 3 mg/L, a few radium isotope activities were desorbed into the water. It indicates that the NO_3^- influences the radium isotope activities and that the Fe-Mn oxides are most capable of desorbing radium isotopes at a NO_3^- of 1 mg/L, which also indicates that the oxidizing properties of oxidants in water can only be optimal under certain conditions (Stefánsson et al., 2005). On the other hand, the response of aqueous radium activity to SO_4^{2-} differed from that of NO_3^-. In spring, the radium activities was mainly distributed in the SO_4^{2-} of 0–6 000 mg/L. The radium isotope activity increased when the SO_4^{2-} was 0–4 500 mg/L. A decreasing trend was reflected in the radium isotope activity once the SO_4^{2-} exceeded 4 500 mg/L.

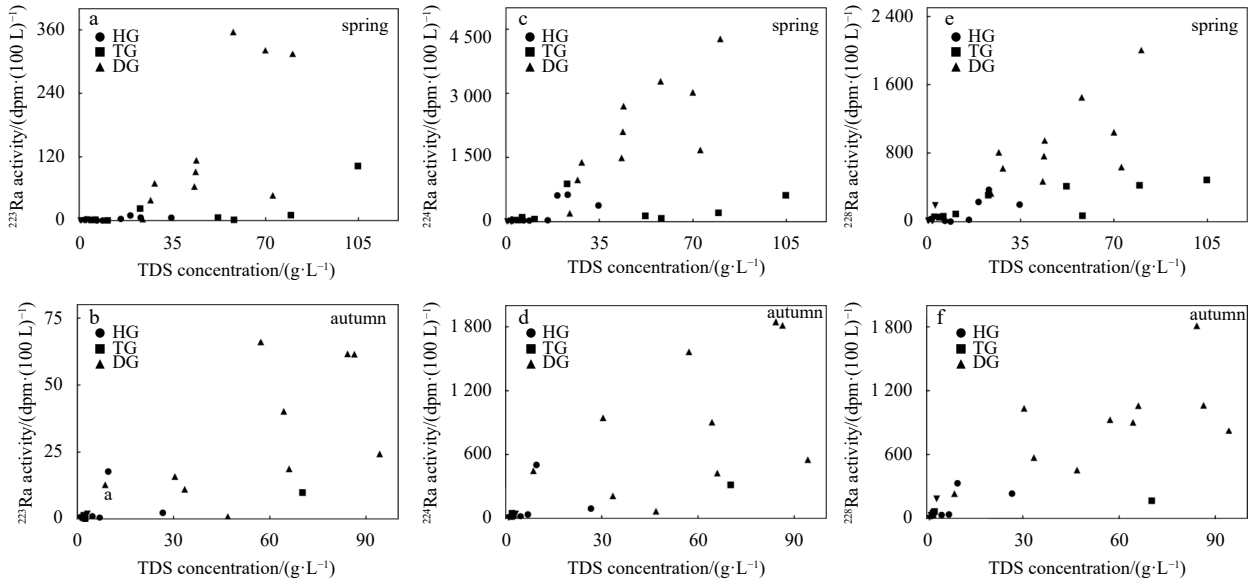

Fig. 6. Different kinds of plots depicting ^{223}Ra (a, b), ^{224}Ra (c, d) and ^{228}Ra (e, f) activities of groundwater (HG: Hangu; TG: Tanggu; DG: Dagang) in relationship with total dissolved solid (TDS) in spring and autumn.

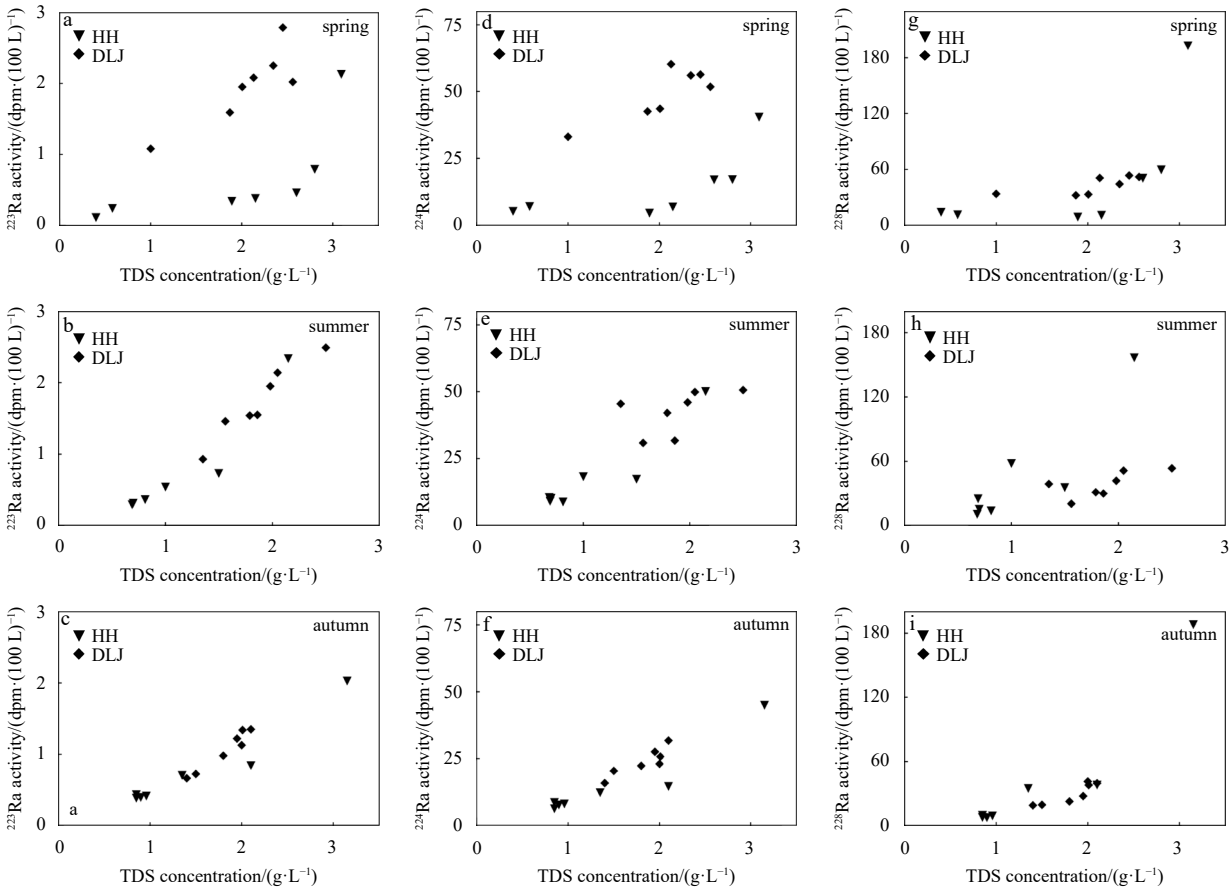

Fig. 7. Different kinds of plots depicting ^{223}Ra (a–c), ^{224}Ra (d–f) and ^{228}Ra (g–i) activities of surface water (HH: Haihe River; DLJ: Duliujian River) in relationship with total dissolved solid (TDS) in spring, summer and autumn.

It indicates that the water column has the most substantial ability to desorb radium isotopes when the SO_4^{2-} is 4 500 mg/L in spring. It is different from the autumn situation. With the increase of SO_4^{2-}, the radium isotope activity in autumn showed an increasing trend, which is an interesting phenomenon. The possible reason is that SO_4^{2-} exhibits a more ionic effect than oxidative due to the season and the acid-base environment of the water column. SO_4^{2-} complexed with Ra^{2+} to form $RaSO_4^0$, which causes the increase of radium isotope activity in the groundwater.

4.3.3 *Hydrogeological conditions*

The HG, TG, and DG profiles on the west coast of Bohai Bay were formed in the Upper Holocene–Middle Holocene (buried depth of about 4–40 m), and Table 5 showed their sediment composition (Pei and Wang, 2016). HG and DG profiles are mainly composed of silty sand (upper layer) and clayey, silty sand (lower layer). In contrast, the TG profile mainly comprises clayey, silty sand (upper layer) and silty sand layer (lower layer).

Stratified and lenticular micro-confined aquifers dominate the shallow groundwater. According to the hydrogeological conditions of the study area, the HG profile (15 m burial depth) is dominated by clayey silt layers. Due to the low percolation rate, the exchange between the upper and lower water bodies is hindered. The TG profile (15 m buried depth) is dominated by clayey silt, while the shell sand layer is dominated at the buried depth of 19 m. A large number of saline substances are accumulated in the shell sand layer, and the high TDS of groundwater in TG is conducive to the desorption of radium isotopes on the surface of the aquifer medium, which may be the main reason for the radium activity of this layer is higher than the buried depth of 30 m. The DG profile (15 m burial depth) mainly comprises clayey silt. It has a low seepage rate and a strong ion exchange capacity between clay with a specific surface area and radium. This further explains why the radium activities of HG, TG, and DG profiles at 15 m depth were higher than that at 30 m depth. Therefore, different aquifers have different lithological characteristics, one of the crucial factors affecting the distribution of radium activity in groundwater (Underwood et al., 2009).

4.3.4 *Seasonal effects*

The average ^{224}Ra/^{228}Ra activity ratio of HG, TG, and DG was 1.12 in spring and autumn, while HH and DLJ were 0.94 in spring, summer, and autumn. It indicates that ^{224}Ra and ^{228}Ra in groundwater and surface water approximated a radiogenic equilibrium with ratios close to 1 (Moore, 2010). Radium activity can be affected by seasonal variation and rainfall processes (Yi et al., 2019). The ^{224}Ra/^{228}Ra activity ratio of groundwater bodies showed a decreasing trend with increasing rainfall from spring to autumn (Fig. 9), which may be due to the lagging effect of the rainfall process. The water with slow vertical velocity has a long residence time. Therefore, ^{224}Ra decays much more than ^{228}Ra simultaneously. In contrast, the radium activities of surface water decreased with rainfall (see Section 3.2).

4.3.5 *Relationship between rapid urbanization and radium activity*

The relationship between rapid urbanization of estuarine and coastal zone in Tianjin and radium isotope is shown in Fig. 10.

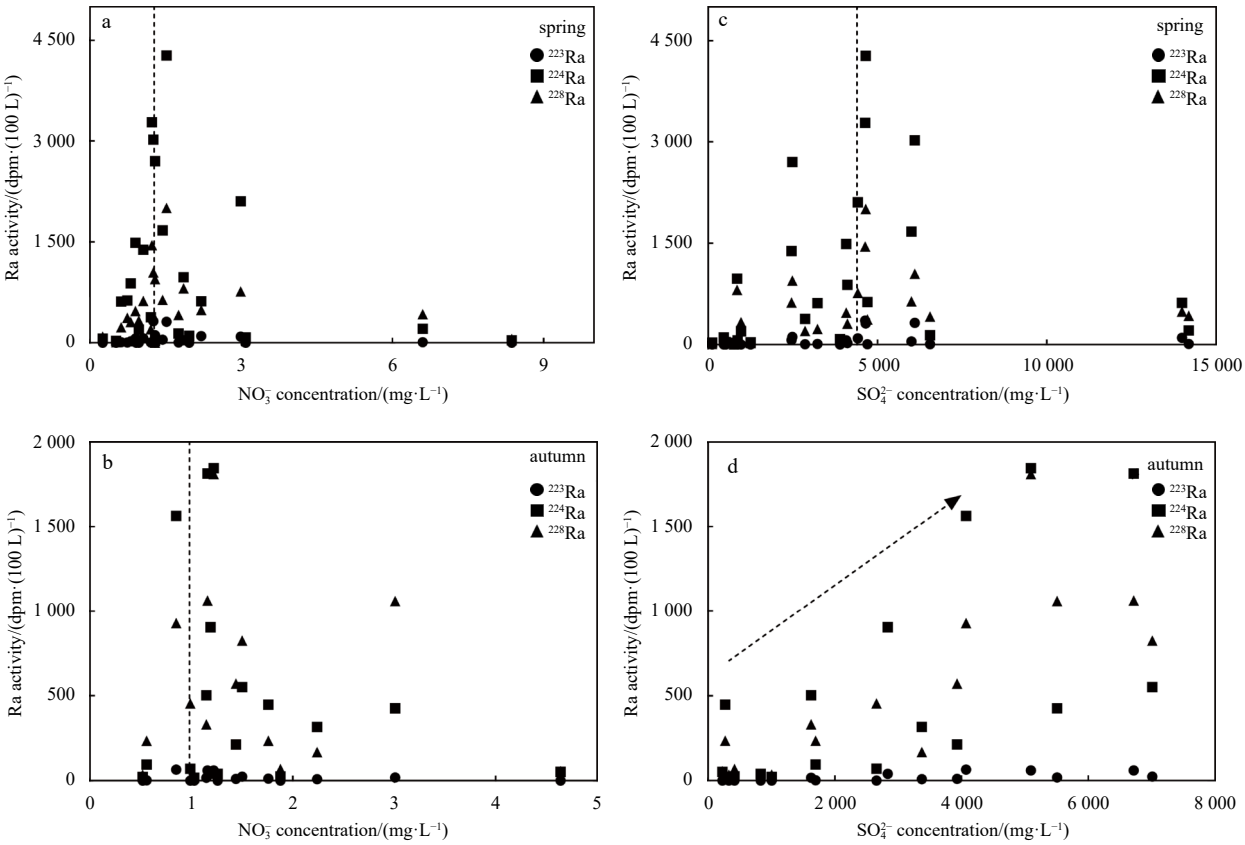

Fig. 8. Different kinds of plots depicting ^{223}Ra, ^{224}Ra and ^{228}Ra activities in relationship with NO_3^- (a, b) and SO_4^{2-} (c, d) in spring and autumn.

Table 5. Stratigraphic division of groundwater (Hangu (HG), Tanggu (TG) and Dagang (DG)) profiles

Study area	Layer bottom elevation/m	Composition of sediments
HG	–9.6	sand silty sand layer
HG	–18.0	silt layer
HG	–19.0	silt layer
HG	–21.0	clay silty sand layer
TG	–18.6	clay silty sand layer
TG	–19.2	shell sand layer
TG	–20.3	clay silty sand layer
TG	–23.0	silt layer
DG	–10.0	clay silty sand layer and fine sand layer
DG	–16.7	clay silty sand layer
DG	–30.2	clay silty sand layer

With the acceleration of urbanization in Tianjin's estuarine and coastal zone, especially since the 1960s, human activities have significantly affected the features of radium isotopes in groundwater and surface water. On the contrary, many scientific studies have shown that radium isotopes can be used as a novel tool to reflect the impact of urbanization on surface water-groundwater systems, for instance, water flushing times (Moore et al., 2006), horizontal and vertical diffusion processes (Moore, 2000a; Ku et al., 1980), exchange processes between surface water and groundwater (Baskaran et al., 2009), and the fluxes of submarine groundwater discharge (SGD) (Moore, 1996).

Features of radium in the surface water (HH and DLJ) are affected by the combined effects of industry and agriculture. Affected by rapid industrial development, the flow of rivers has been at a low level, and the accumulation of sediments and suspended particles in the river is severe, which reduces the activities of radium in HH and DLJ (Lei et al., 2007). Additionally, the waterway dredging changed the topography of HH and DLJ, and the reduction of the shallow intertidal zone allowed the sediment to be resuspended, the variable environment complicates the diffusion of radium isotopes on suspended matter (Wu et al., 2005). The discharge of large amounts of nutrients (NO_3^-, NO_2^-, and SO_4^{2-}) from coastal domestic and farming wastewater has led to severe eutrophication of HH and DLJ, which was consistent with the previous study (Cao and Corriveau, 2008). This phenomenon alters the redox environment of the water column, which in turn affects the distribution of radium isotopes.

Unlike surface water, groundwater in the three regions (HG, TG and DG) faces severe challenges. For example, the large-scale land reclamation has changed the groundwater level and seriously hindered the runoff and discharge of groundwater, which may affect the exchange of surface water and groundwater and the inaccuracy of SGD flux assessment by radium isotopes (Jiao et al., 2008; Nie and Tao, 2009). Tang et al. (2015) also indicated that the land use pattern was one of the major factors controlling the features of radium in this area. Due to the over-exploitation of groundwater, the groundwater tables of HG and TG decreased significantly, which would change the groundwater runoff and further affect the migration behavior of radium isotopes (Yi et al., 2011). The activities of radium in DG were much higher than that in the HG and TG regions, which may be related to the oil exploration and production in this area. Liu et al. (2007) indicated that over 50 years of oil exploration have caused severe pollution of shallow groundwater in DG, and radium isotope is one of the

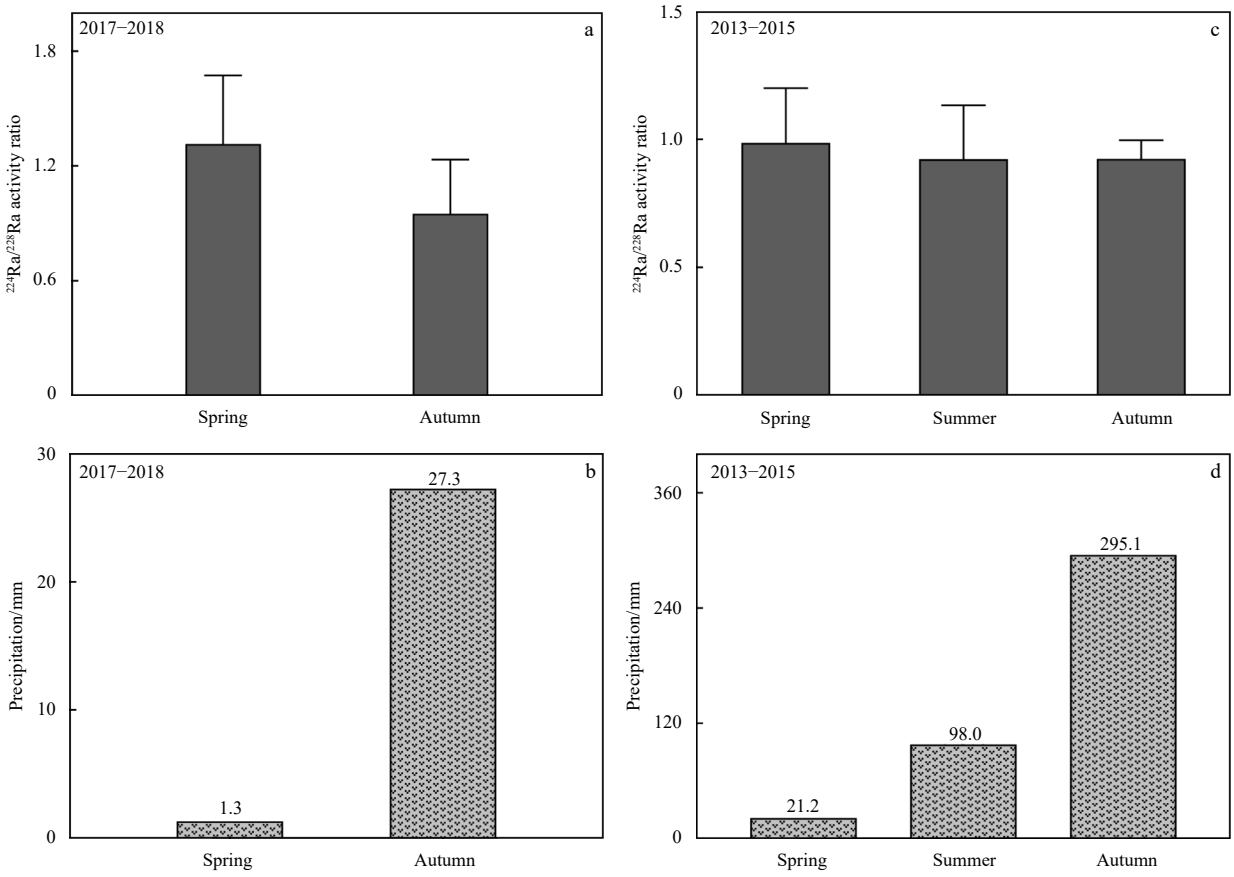

Fig. 9. Relationship between $^{224}Ra/^{228}Ra$ isotope activity ratio and precipitation (mm) under different seasonal variations in groundwater (a, b) and surface water (c, d).

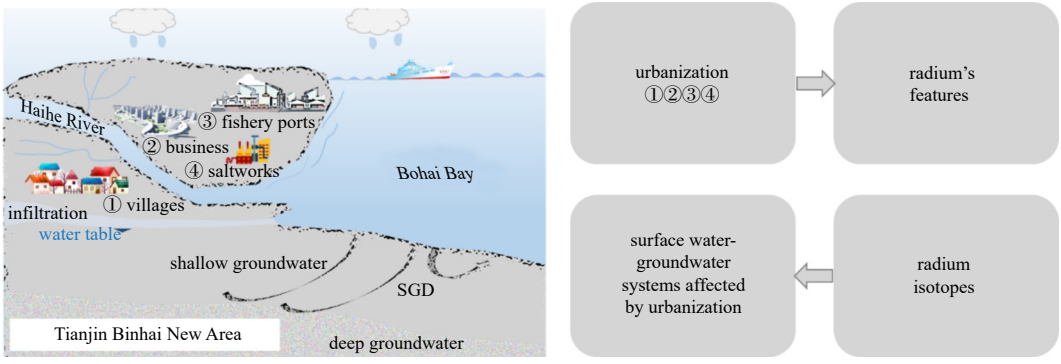

Fig. 10. Relationship between rapid urbanization and radium isotopes in Tianjin Binhai New Area. SGD: submarine groundwater discharge.

common radioactive elements in petroleum exploitation by-products (Parmaksız et al., 2015).

In addition, agriculture, animal husbandry, tourism and high-tech industries (marine bioengineering and electronic engineering) may also directly or indirectly affect the features of radium isotopes in the surface water-groundwater system (Pulido-Bosch et al., 2018; Silva and Mattos, 2020). Therefore, rapid urbanization will inevitably affect the source, transport, fate, and distribution of radium isotopes in surface water and groundwater in estuarine and coastal zone.

On the other hand, radium isotopes can be used to reflect the impact of urbanization on surface water-groundwater systems. For example, the "radium isotope (^{223}Ra and ^{224}Ra) apparent age model" proposed by Moore (1996) was used in this study to calculate the water residence time of groundwater (HG, TG and DG). The results showed that the average residence time of HG, TG and DG in spring is 11.50 d, 15.50 d and 18.80 d, respectively, which is higher than 11.36 d, 14.99 d and 15.73 d in autumn. It may be that the rainfall in spring is lower than that in autumn, and the rainfall process accelerates the flow of groundwater (Yi et al., 2019). In addition, the research on the application of radium isotopes to SGD is based on the principle of mass balance model, assuming that the region is in a stable state, and the calculation of SGD fluxes is completed through the source and sink terms of radium isotopes (Moore, 1996). In summary, this study suggests that correctly viewing and clarifying the relationship between ra-

dium isotopes and urbanization will help better understand the regional hydrogeochemical processes and the sweet development of the Tianjin's estuarine and coastal zone.

5 Conclusions

The estuarine and coastal area is the crucial area of material exchange between land and ocean. The features and factors of radium isotope activity in groundwater and surface water in Tianjin Binhai New Area were analyzed. The main conclusions are as follows:

(1) Radium activity (HG, TG, and DG) and spatial variability in groundwater were higher than those in surface water (HH and DLJ). Radium activity in groundwater increased from north to south. The radium activity of HG and TG showed an increasing trend from inland to the coastline, but the radium activities of DG increased first and then decreased. The radium activity at 15 m depth was higher than at 30 m depth. Radium activity in surface water also increased from inland to the coastline.

(2) High TDS promoted the desorption of radium adsorbed on the surface of particulate matter, enhancing the radium activity of groundwater and surface water, but the desorption rates were different. Nitrate affects the activity of radium, and when its concentration was 1 mg/L, the Fe-Mn oxide had the most substantial desorption ability to the radium isotope. The desorption of radium isotopes by Fe-Mn oxides was strong in spring when SO_4^{2-} was 4 500 mg/L. There was a consistent trend of increasing radium activity in autumn, influenced by seasonal variation and acid-base environments, and SO_4^{2-} showed ionic effects rather than oxidative.

(3) The radium activity in spring was higher than in autumn, and the radium activity of surface water decreased with increasing rainfall. The $^{224}Ra/^{228}Ra$ activity ratio of groundwater showed a decreasing trend due to the lagging effect of the rainfall process.

(4) Rapid urbanization will inevitably affect the features of radium isotopes in surface water and groundwater in estuarine and coastal zone. Meanwhile, radium isotopes can be used to reflect the impact of urbanization on surface water-groundwater systems.

References

Abboud I A. 2018. Geochemistry and quality of groundwater of the Yarmouk basin aquifer, north Jordan. Environmental Geochemistry and Health, 40(4): 1405–1435, doi: 10.1007/s10653-017-0064-x

Adelana S M, Heaven M W, Dresel P E, et al. 2020. Controls on species distribution and biogeochemical cycling in nitrate-contaminated groundwater and surface water, southeastern Australia. Science of the Total Environment, 726: 138426, doi: 10.1016/j.scitotenv.2020.138426

Baskaran S, Ransley T, Brodie R S, et al. 2009. Investigating groundwater–river interactions using environmental tracers. Australian Journal of Earth Sciences, 56(1): 13–19, doi: 10.1080/08120090802541887

Beck A J, Cochran M A. 2013. Controls on solid-solution partitioning of radium in saturated marine sands. Marine Chemistry, 156: 38–48, doi: 10.1016/j.marchem.2013.01.008

Beck A J, Rapaglia J P, Cochran J K, et al. 2007. Radium mass-balance in Jamaica Bay, NY: evidence for a substantial flux of submarine groundwater. Marine Chemistry, 106(3–4): 419–441, doi: 1016/j.marchem.2007.03.008

Cao Xuliang, Corriveau J. 2008. Migration of bisphenol A from polycarbonate baby and water bottles into water under severe conditions. Journal of Agricultural and Food Chemistry, 56(15): 6378–6381, doi: 10.1021/jf800870b

Charette M A, Morris P J, Henderson P B, et al. 2015. Radium isotope distributions during the US GEOTRACES North Atlantic cruises. Marine Chemistry, 177: 184–195, doi: 10.1016/j.marchem.2015.01.001

Charette M A, Sholkovitz E R. 2002. Oxidative precipitation of groundwater-derived ferrous iron in the subterranean estuary of a coastal bay. Geophysical Research Letters, 29(10): 1444, doi: 10.1029/2001g104512

Charette M A, Sholkovitz E R. 2006. Trace element cycling in a subterranean estuary: Part 2. Geochemistry of the pore water. Geochimica et Cosmochimica Acta, 70(4): 811–826, doi: 10.1016/j.gca.2005.10.019

Chen Guangquan, Xu Bochao, Zhao Shibin, et al. 2022. Submarine groundwater discharge and benthic biogeochemical zonation in the Huanghe River Estuary. Acta Oceanologica Sinica, 41(1): 11–20, doi: 10.1007/s13131-021-1882-3

Elsinger R J, Moore W S. 1980. ^{226}Ra behavior in the Pee Dee River-Winyah Bay estuary. Earth and Planetary Science Letters, 48(2): 239–249, doi: 10.1016/0012-821X(80)90187-9

Garcia-Orellana J, Rodellas V, Tamborski J, et al. 2021. Radium isotopes as submarine groundwater discharge (SGD) tracers: review and recommendations. Earth-Science Reviews, 220: 103681, doi: 10.1016/j.earscirev.2021.103681

Giggenbach W F. 1988. Geothermal solute equilibria. Derivation of Na-K-Mg-Ca geoindicators. Geochimica et Cosmochimica Acta, 52(12): 2749–2765, doi: 10.1016/0016-7037(88)90143-3

Gonneea M E, Morris P J, Dulaiova H, et al. 2008. New perspectives on radium behavior within a subterranean estuary. Marine Chemistry, 109(3–4): 250–267, doi: 10.1016/j.marchem.2007.12.002

Grundl T, Cape M. 2006. Geochemical factors controlling radium activity in a sandstone aquifer. Groundwater, 44(4): 518–527, doi: 10.1111/j.1745-6584.2006.00162.x

IAEA. 2014. The environmental behaviour of radium: revised edition. Vienna: International Atomic Energy Agency, 33–51

Jiao Jiu-jimmy, Leung Chi-man, Ding Guoping. 2008. Changes to the groundwater system, from 1888 to present, in a highly-urbanized coastal area in Hong Kong, China. Hydrogeology Journal, 16(8): 1527–1539, doi: 10.1007/s10040-008-0332-z

Kelly R P, Moran S B. 2002. Seasonal changes in groundwater input to a well-mixed estuary estimated using radium isotopes and implications for coastal nutrient budgets. Limnology and Oceanography, 47(6): 1796–1807, doi: 10.4319/lo.2002.47.6.1796

Kiro Y, Yechieli Y, Voss C I, et al. 2012. Modeling radium distribution in coastal aquifers during sea level changes: the Dead Sea case. Geochimica et Cosmochimica Acta, 88: 237–254, doi: 10.1016/j.gca.2012.03.022

Krest J M, Harvey J W. 2003. Using natural distributions of short-lived radium isotopes to quantify groundwater discharge and recharge. Limnology and Oceanography, 48(1): 290–298, doi: 10.4319/lo.2003.48.1.0290

Ku T L, Huh C A, Chen P S. 1980. Meridional distribution of ^{226}Ra in the eastern Pacific along GEOSECS cruise tracks. Earth and Planetary Science Letters, 49(2): 293–308, doi: 10.1016/0012-821X(80)90073-4

Langmuir D, Melchior D. 1985. The geochemistry of Ca, Sr, Ba and Ra sulfates in some deep brines from the Palo Duro Basin, Texas. Geochimica et Cosmochimica Acta, 49(11): 2423–2432, doi: 10.1016/0016-7037(85)90242-X

Lei Kun, Meng Wei, Zheng Binghui, et al. 2007. Variations of water and sediment discharges to the western coast of Bohai Bay and the environmental impacts. Acta Scientiae Circumstantiae (in Chinese), 27(12): 2052–2059

Liao Fu, Wang Guangcai, Yi Lixin, et al. 2020. Applying radium isotopes to estimate groundwater discharge into Poyang Lake, the largest freshwater lake in China. Journal of Hydrology, 585: 124782, doi: 10.1016/j.jhydrol.2020.124782

Liu Rongfang, Chen Honghan, Wang Yanliang, et al. 2007. Analysis on characteristics of groundwater pollution in the oilfield. Ground Water (in Chinese), 29(3): 62–66

Liu Huatai, Guo Zhanrong, Gao Aiguo, et al. 2013. Distribution characteristics of radium and determination of transport rate in the Min River Estuary Mixing Zone. Journal of Jilin University:

Earth Science Edition (in Chinese), 43(6): 1966–1971
Liu Yi, Jiao Jiu-jimmy, Mao Rong, et al. 2019. Spatial characteristics reveal the reactive transport of radium isotopes (^{224}Ra, ^{223}Ra, and ^{228}Ra) in an intertidal aquifer. Water Resources Research, 55(12): 10282–10302, doi: 10.1029/2019WR024849
Liu Lingling, Yi Lixin, Cheng Xiaoqing, et al. 2015. Distribution of ^{223}Ra and ^{224}Ra in the Bo Sea embayment in Tianjin and its implication of submarine groundwater discharge. Journal of Environmental Radioactivity, 150: 111–120, doi: 10.1016/j.jenvrad.2015.08.008
Lu Xinyan, Yi Lixin, Pu Tao, et al. 2022. Quantifying the groundwater seepage along a glacier originated river by integrated use of radium isotopes and hydrochemistry. Journal of Environmental Radioactivity, 251–252: 106959, doi: 10.1016/j.jenverad.2022.106959
Luo Xin, Jiao Jiu-jimmy, Moore W S, et al. 2014. Submarine groundwater discharge estimation in an urbanized embayment in Hong Kong via short-lived radium isotopes and its implication of nutrient loadings and primary production. Marine Pollution Bulletin, 82(1–2): 144–154, doi: 10.1016/j.marpolbul.2014.03.005
Moore W S. 1996. Large groundwater inputs to coastal waters revealed by ^{226}Ra enrichments. Nature, 380(6575): 612–614, doi: 10.1038/380612a0
Moore W S. 2000a. Determining coastal mixing rates using radium isotopes. Continental Shelf Research, 20(15): 1993–2007, doi: 10.1016/S0278-4343(00)00054-6
Moore W S. 2000b. Ages of continental shelf waters determined from ^{223}Ra and ^{224}Ra. Journal of Geophysical Research: Oceans, 105(C9): 22117–22122, doi: 10.1029/1999JC000289
Moore W S. 2008. Fifteen years experience in measuring ^{224}Ra and ^{223}Ra by delayed-coincidence counting. Marine Chemistry, 109(3–4): 188–197, doi: 10.1016/j.marvhem.2007.06.015
Moore W S. 2010. The effect of submarine groundwater discharge on the ocean. Annual Review of Marine Science, 2: 59–88, doi: 10.1146/annurev-marine-120308-081019
Moore W S, Arnold R. 1996. Measurement of ^{223}Ra and ^{224}Ra in coastal waters using a delayed coincidence counter. Journal of Geophysical Research: Oceans, 101(C1): 1321–1329, doi: 10.1029/95JC03139
Moore W S, Astwood H, Lindstrom C. 1995. Radium isotopes in coastal waters on the Amazon shelf. Geochimica et Cosmochimica Acta, 59(20): 4285–4298, doi: 10.1016/0016-7037(95)00242-R
Moore W S, Blanton J O, Joye S B. 2006. Estimates of flushing times, submarine groundwater discharge, and nutrient fluxes to Okatee Estuary, South Carolina. Journal of Geophysical Research, 111(C9): C09006, doi: 10.1029/2005jc003041
Moore W S, Key R M, Sarmiento J L. 1985. Techniques for precise mapping of ^{226}Ra and ^{228}Ra in the ocean. Journal of Geophysical Research: Oceans, 90(C4): 6983–6994, doi: 10.1029/JC090iC04p06983
Nie Hongtao, Tao Jianhua. 2009. Eco-environment status of the Bohai Bay and the impact of coastal exploitation. Marine Science Bulletin, 11(2): 81–96
Parmaksız A, Ağuş Y, Bulgurlu F, et al. 2015. Measurement of enhanced radium isotopes in oil production wastes in Turkey. Journal of Environmental Radioactivity, 141: 82–89, doi: 10.1016/j.jenvrad.2014.12.011
Pei Yandong, Wang Guoming. 2016. Engineering geological characteristics of Late Quaternary sediments in the southern coastal area of Tianjin Binhai New Area. Geological Survey and Research (in Chinese), 39(3): 215–220
Plater A J, Ivanovich M, Dugdale R E. 1995. ^{226}Ra contents and ^{228}Ra/^{226}Ra activity ratios of the Fenland rivers and the Wash, eastern England: spatial and seasonal trends. Chemical Geology, 119(1–4): 275–292, doi: 10.1016/0009-2541(94)00109-1
Pulido-Bosch A, Rigol-Sanchez J P, Vallejos A, et al. 2018. Impacts of agricultural irrigation on groundwater salinity. Environmental Earth Sciences, 77(5): 197, doi: 10.1007/s12665-018-7386-6
Shao Haibing, Kulik D A, Berner U, et al. 2009. Modeling the competition between solid solution formation and cation exchange on the retardation of aqueous radium in an idealized bentonite column. Geochemical Journal, 43(6): e37–e42, doi: 10.2343/geochemj.1.0069
Sherif M I, Lin Jiajia, Poghosyan A, et al. 2018. Geological and hydrogeochemical controls on radium isotopes in groundwater of the Sinai Peninsula, Egypt. Science of The Total Environment, 613–614: 877–885, doi: 10.1016/j.scitotenv.2017.09.129
Silva K B, Mattos J B. 2020. A spatial approach for the management of groundwater quality in tourist destinations. Tourism Management, 79: 104079, doi: 10.1016/j.tourman.2020.104079
Stefánsson A, Arnórsson S, Sveinbjörnsdóttir Á E. 2005. Redox reactions and potentials in natural waters at disequilibrium. Chemical Geology, 221(3–4): 289–311, doi: 10.1016/j.chemgeo.2005.06.003
Su Ni, Du Jinzhou, Liu Sumei, et al. 2013. Nutrient fluxes via radium isotopes from the coast to offshore and from the seafloor to upper waters after the 2009 spring bloom in the Yellow Sea. Deep-Sea Research Part II: Topical Studies in Oceanography, 97: 33–42, doi: 10.1016/j.dsr2.2013.05.003
Sun Congjian, Chen Ruoxia, Zhang Ziyu, et al. 2018. Temporal and spatial variation of hydrochemical characteristics of shallow groundwater in Shanxi Province. Arid Land Geography (in Chinese), 41(2): 314–324
Tang Guoqiang, Yi Lixin, Liu Lingling, et al. 2015. Factors influencing the distribution of ^{223}Ra and ^{224}Ra in the coastal waters off Tanggu and Qikou in Bohai Bay. Continental Shelf Research, 109: 177–187, doi: 10.1016/j.csr.2015.09.003
Trainer F W, Heath R C. 1976. Bicarbonate content of groundwater in carbonate rock in eastern North America. Journal of Hydrology, 31(1–2): 37–55, doi: 10.1016/0022-1694(76)90019-6
Underwood E C, Ferguson G A, Betcher R, et al. 2009. Elevated Ba concentrations in a sandstone aquifer. Journal of Hydrology, 376(1–2): 126–131, doi: 10.1016/j.jhydrol.2009.07.019
van der Loeff M R, Kühne S, Wahsner M, et al. 2003. ^{228}Ra and ^{226}Ra in the Kara and Laptev seas. Continental Shelf Research, 23(1): 113–124, doi: 10.1016/S0278-4343(02)00169-3
Vinson D S, Tagma T, Bouchaou L, et al. 2013. Occurrence and mobilization of radium in fresh to saline coastal groundwater inferred from geochemical and isotopic tracers (Sr, S, O, H, Ra, Rn). Applied Geochemistry, 38: 161–175, doi: 10.1016/j.apgeochem.2013.09.004
Waska H, Kim S, Kim G, et al. 2008. An efficient and simple method for measuring ^{226}Ra using the scintillation cell in a delayed coincidence counting system (RaDeCC). Journal of Environmental Radioactivity, 99(12): 1859–1862, doi: 10.1016/j.jenvrad.2008.08.008
Wu Yinghai, Zhu Weibin, Chen Xiaohua, et al. 2005. Effects of enclosing-bank and hydraulic fill projects on water environment. Water Resources Protection (in Chinese), 21(2): 53–56
Xiao Qingcong, Wei Yuansong, Wang Yawei, et al. 2012. Driving factors of coastal wetland degradation in Binhai New Area of Tianjin. Acta Scientiae Circumstantiae (in Chinese), 32(2): 480–488
Yi Lixin, Dong Na, Zhang L, et al. 2019. Radium isotopes distribution and submarine groundwater discharge in the Bohai Sea. Groundwater for Sustainable Development, 9: 100242, doi: 10.1016/j.gsd.2019.100242
Yi Lixin, Zhang Fang, Xu He, et al. 2011. Land subsidence in Tianjin, China. Environmental Earth Sciences, 62(6): 1151–1161, doi: 10.1007/s12665-010-0604-5